Long Term Behavior of Geogrids in Reinforced Clay Slopes

Y. Liu, J. D. Scott & D. C. Sego
University of Alberta, Edmonton, AB, Canada

ABSTRACT

Long term behavior of polymeric geogrids is one of the major concerns in designing reinforced slopes and walls. It is commonly considered that the strength and stiffness of the geogrids decrease due to aging and environmental deterioration. In addition to laboratory creep test results, the aging under field conditions and environmental deterioration of polymer materials can be effectively studied by analyzing case histories. Tensile strains developed in geogrids were measured in reinforced cohesive soil slopes in an instrumented test embankment, 12 m high with 1:1 side slopes. The field measurements of the geogrid strains, for three years during construction and for four years thereafter, indicate that the time-dependent tensile strains in the geogrids were insignificant.

Keywords: reinforced slopes, geogrid strains, field measurements, long term

INTRODUCTION

Geogrids have been used extensively for soil reinforcement purposes in geotechnical engineering. The placement of reinforcement increases the soil resistance and reduces cracking and localized failures within the soil structures. The reinforcing function of the geogrids depends upon the tensile resistance of the geogrids which is mobilized through shear between the soil and the members of the reinforcement. In design of a reinforced soil slope, the tensile resistance from the reinforcement is incorporated into a stability analysis, often using a limit equilibrium method (Jewell, 1991). The magnitude of the tensile resistance is usually determined based on the anticipated tensile strains which would develop in the geogrids as the soil mass deforms. Due to the nature of polymeric materials, long term behavior of the geogrids is a major concern to designers (Fannin and Hermann 1991, Jewell and Greenwood 1988, Koerner 1990 and McGown *et al.* 1984). In addition to laboratory creep test results, direct field measurements of geogrid strains in reinforced soil structures are essential in evaluating the long term performance of the geogrids under field conditions.

A test embankment, 12 m high with 1:1 side slopes, was built near Devon, Alberta, Canada (Liu *et al.*, 1991). It has four slope sections, three are reinforced with different types of geogrid and the fourth slope is unreinforced for comparison (Figure 1). The primary objective of constructing the test embankment was to analyze the reinforcing mechanisms of the geogrids and to determine the stress distribution within the cohesive soil embankment. An additional objective was to compare the performance of three different geogrid materials and to evaluate appropriate construction procedures to build geogrid reinforced slopes. In order to study the stress transfer from the soil to the geogrids during the construction of the embankment, the test slopes were designed with an initial low factor of safety to encourage the development of lateral strain in the soil to mobilize the tensile resistance of the geogrids. To ensure that lateral strains would occur and to ensure that each reinforcing layer would act independently, only three primary reinforcing layers at a 2 m vertical spacing were installed in the test fill (Figure. 2).

This paper presents the field measurements of the geogrids strains in the reinforced slopes. Due to defects in the manufacturing of the square grid materials installed in the test embankment, the strains which developed in this geogrid were highly localized so that the overall behavior of the square grid reinforced slope was similar to the unreinforced slope. Hence, the performance of this geogrid will not be discussed separately.

TEST EMBANKMENT

The test embankment was founded on glaciolacustrine sediments. The top 4 m of the foundation soil is a silty clay at an average natural water content of 32%. The ground water table was 5 m below the ground surface. In order to generate sufficient tensile strains in the geogrids, the silty clay, which was relatively soft, was used as the material to construct the embankment. The soil is composed of 25% sand, 50% silt and 25% clay sizes. It is described as an inorganic clay of low to medium plasticity as the liquid limit and plastic limit of the fill soil are 42% and 18% respectively. Standard compaction tests indicated that the optimum water content is approximately 21.5% and the corresponding maximum dry density is 1,600 kg/m^3. Consolidated undrained triaxial shear tests with pore pressure measurements were conducted on the compacted fill soil. Typically, the soil exhibited strain strengthening behavior. In most cases, the principal effective stress ratio reached a maximum value at axial strains of about 12%. The tests gave an average effective friction angle of 28 degrees and an effective cohesion range from 8 to 14 kPa.

Three types of geogrids were used as reinforcing materials in the test embankment. The physical properties of the geogrids are summarized in Table 1 and the results of wide strip tensile tests are shown in Figure 3.

The test embankment was constructed in three stages. The construction started in September 4 (day 0) 1986 and the embankment reached a height of 3 m at the end of the first construction season in October, 1986. The bottom primary reinforcing geogrid layer was placed 1 m above the ground surface in the first season. During the second construction season in 1987, an additional 3 m of fill was placed and the middle and top layers of primary reinforcing geogrids were installed at 3 and 5 m above the ground surface. The test fill construction was completed to the designed 12 m height in October, 1988.

The strains in the geogrids were monitored using electrical inductance coils and electrical wire resistance strain gauges (EWR). The instrumented positions start at 0.5 m from the slope surface and then at 1 m intervals beyond the 1 m location. At each instrumented location, a pair of EWR strain gauges were bonded to a longitudinal member of the geogrid to measure the strains induced in the longitudinal member while a pair of electric inductance coils were attached at the same location to monitor the deformations between adjacent transverse members. A thermocouple was placed at each instrumented position to account for the influence of temperature on the strain measurements. The temperature induced strains in the EWR gauges were calculated as the product of the thermal expansion coefficients of the geogrids, obtained in laboratory thermal expansion tests, and the temperature differences measured in the field using the thermocouples; they were subtracted from the measured total strains, resulting in strains developed in a geogrid due only to the loading transferred from the soil.

MEASUREMENTS OF GEOGRID STRAINS

Strains in the geogrids were measured using electrical inductance coils and electrical wire resistance strain gauges (EWR). It was found that the distributions of the geogrid strains from the two types of measurements were similar to each other; the magnitudes of the strains, however, were often different. From the analysis of the field measurements, it appeared that the EWR gauge strains were more consistent and meaningful; they could also be directly related to standard tensile load tests carried out on geogrids when loads in geogrids are of interest. The geogrid strains presented in this paper were from the EWR gauge measurements.

The profiles of the uniaxial and rectangular geogrid strains at the end of the construction are illustrated in Figure 4. All profiles show similar characteristics in strain distribution. Typically, the tensile strain in the reinforcement increases from zero at the slope surface to a maximum at a certain depth and then decreases as the distance from the slope surface increases. In the uniaxial grid reinforced slope, the top layer of the geogrid had the largest strain and the bottom layer had the smallest. In the rectangular grid reinforced slope, the strains developed in the three reinforcing layers were of similar magnitudes. It was also noted that the peak strains in the uniaxial geogrids occurred closer to the slope surface than in the rectangular geogrids. The differences in the strain distributions are mainly related to the differences in geometrical and mechanical properties of the two types of geogrids (Liu, 1992).

Figure 4 shows the development of tensile strains in the uniaxial geogrids during three years of fill construction and four years after construction. The strain development in the rectangular grid layers is shown in Figure 6. The tensile strains in the geogrids increased during the construction seasons and decreased slightly through the winter before the next construction season. There were significant increases in the geogrid strains during the 1988 construction season when additional 6 m of soil was placed in two months. The tensile strains then remained virtually unchanged, except seasonal fluctuations, over four years after completion of the construction. No time-dependent strains have been observed in both the uniaxial grid and the rectangular grid for construction induced tensile strains less than 3%. It is seen from the plots that the strains fluctuated less deep in the fill than near the slope surface. These fluctuations were most likely caused by problems related to the corrections applied to the apparent thermal strains (Liu, 1992).

CONCLUSIONS

The characteristics of the tensile strain distribution along the geogrids are similar in different geogrid layers. The strain increased from zero at the slope surface to a

maximum and then decreased with distance from the slope surface. At the end of construction when the fill height was 12 m, the maximum tensile strains were 2.8% for the uniaxial geogrid and 2% for the rectangular geogrid. In the uniaxial grid reinforced slope, the top layer developed the largest strain while the bottom layer had the smallest. In the rectangular grid reinforced slope, the three primary reinforcing layers developed maximum tensile strains of similar magnitudes.

Within a period of four years after completion of the embankment, no significant time-dependent strains were measured in the longitudinal members in either the uniaxial or the rectangular geogrids.

Geogrid	Uniaxial Grid	Rectangular Grid	Square Grid
Product	Tensar SR2	Signode TNX5001	Paragrid 50S
Type of Polymer	high density polyethylene	polyester	polyester polypropylene
Junction	planar	welded	welded
Weight (g/m^3)	930	544	530
Open Area (%)	55	58	78
Aperture Size (mm)	MD99.1, CMD15.2	MD89.7, CMD26.2	MD66.2, CMD66.2
Thickness (mm)	T 1.27 A 4.57	T 0.75 J 1.5	T 2.5 J 3.75
Color	black	black	yellow
MD: machine direction; CMD: cross machine direction; T: Longitudinal (tension) member; A: Latitudinal (anchor) member; J: joint			

Table 1. Properties of Geogrids

ACKNOWLEDGEMENTS

Alberta Transportation and Utilities funded this research project. The assistance from the Geotechnical Section and Research and Development Branch and District 7 of Alberta Transportation and Utilities is greatly appreciated.

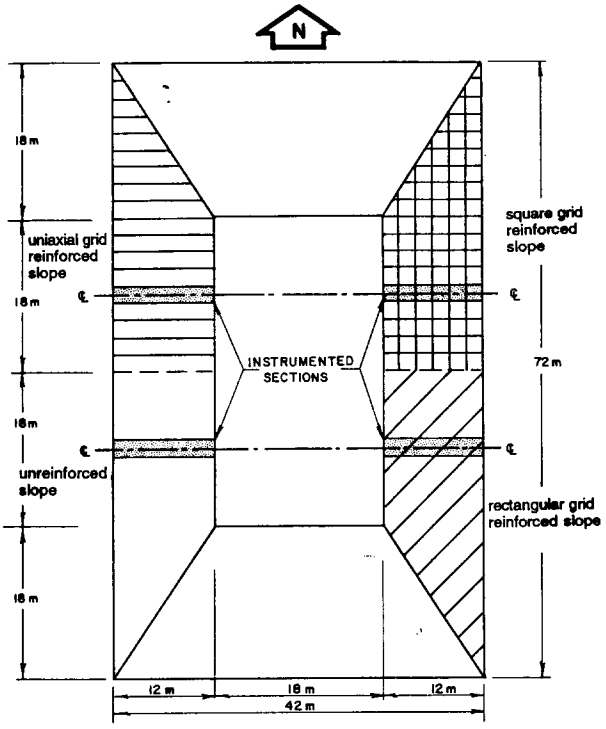

Figure 1. Plan View of Test Embankment

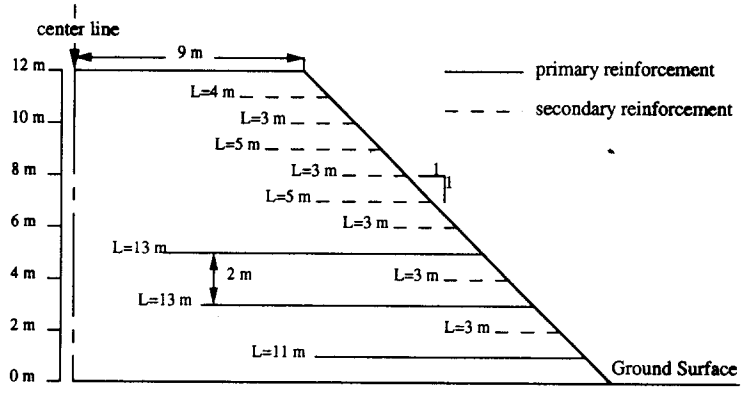

Figure 2. Geogrid Layout in Reinforced Slopes

REFERENCES

Fannin, R.J. and Hermann, S. 1991. Creep Measurements of Polymeric Reinforcement. Proc. of Geosynthetics Conference '91, Atlanta, Vol. 2, pp. 561-573

Jewell, R.A. 1991. Application of Revised Design Charts for Steep Reinforced Slopes. *Geotextiles and Geomembranes*, Vol. 10, pp. 203-233

Jewell, R.A. and Greenwood, J.H. 1988. Long Term Strength and Safety in Steep Soil Slopes Reinforced by Polymer Materials. *Geotextiles and Geomembranes*, Vol. 7, pp. 237-273

Koerner, R.M. 1990. **Design with Geosynthetics**. 2nd Edition, Prentice Hall, New York, 652 p.

Liu, Y. 1992. Performance of Geogrid Reinforced Clay Slopes. Ph.D thesis, Department of Civil Engineering, University of Alberta, Edmonton, Canada, 406 p.

Liu, Y., Scott, J.D., Sego, D.C. and Diyaljee, V. 1991. Performance of Geogrid Reinforced Test Fill. 44th Canadian Geotechnical Conference, Calgary, Vol. 2, pp. 79.1-79.10

McGown, A., Andrawes, K.Z. and Yeo, K.C. 1984. The Load-Strain-Time Behavior of Tensar Geogrids. Proceedings of Conference on Polymer Grid Reinforcement, London, pp. 31-36

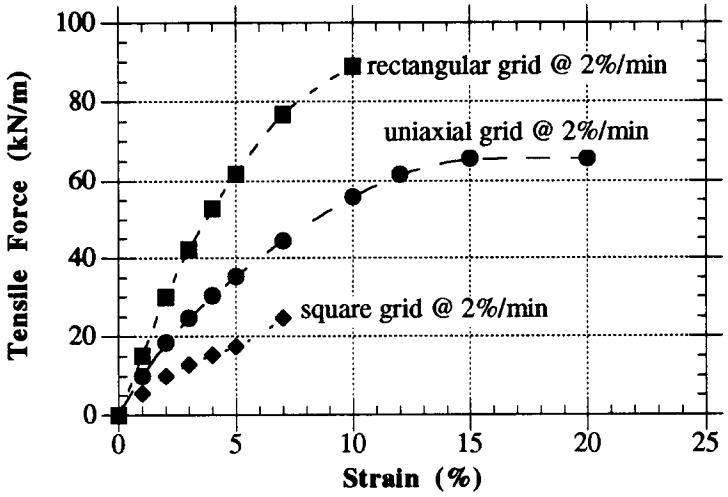

Figure 3. Wide Strip Tensile Test Results

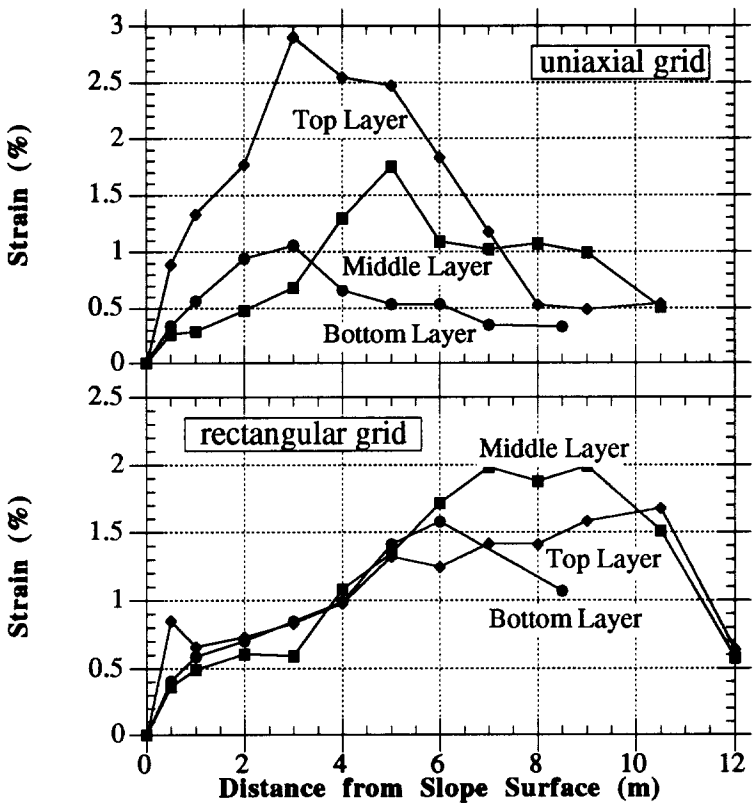

Figure 4. Tensile Strain Distribution in Geogrids

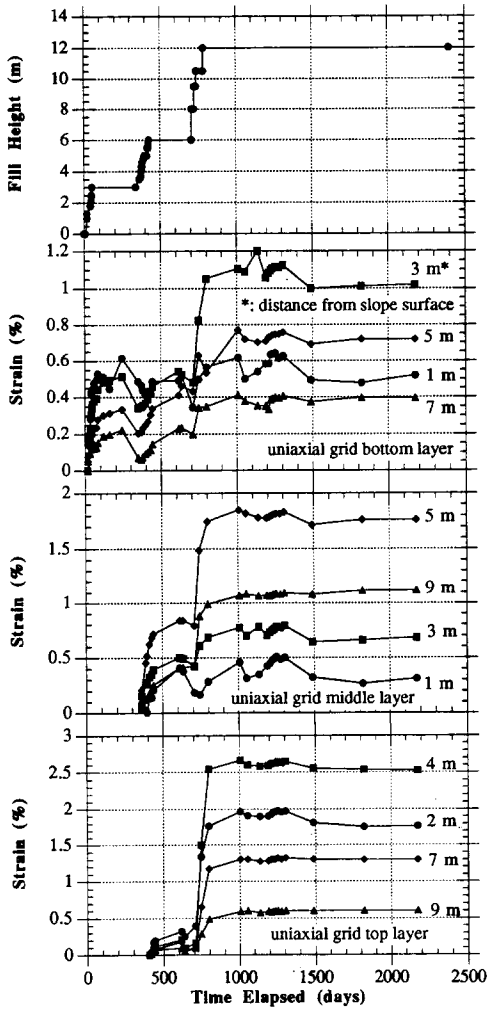

Figure 5. Development of Strains in Uniaxial Grid

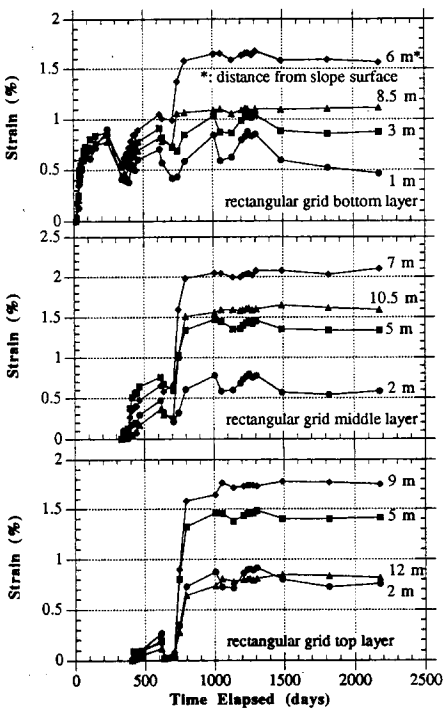

Figure 6. Development of Strains in Retangular Grid